$REPt_3Si$ (RE = La, Pr, Nd, Sm and Gd): isotypes of the heavy fermion superconductor $CePt_3Si$

2005 J. Phys.: Condens. Matter 17 1877

(http://iopscience.iop.org/0953-8984/17/12/012)

INSTITUTE OF PHYSICS PUBLISHING JOURNAL OF PHYSICS: CONDENSED MATTER

J. Phys.: Condens. Matter **17** (2005) 1877–1888 doi:10.1088/0953-8984/17/12/012

$REPt_3Si$ (RE = La, Pr, Nd, Sm and Gd): isotypes of the heavy fermion superconductor $CePt_3Si$

E Bauer[1,5], R Lackner[1], G Hilscher[1], H Michor[1], M Sieberer[1], A Eichler[2], A Gribanov[3], Y Seropegin[3] and P Rogl[4]

[1] Institute of Solid State Physics, Vienna University of Technology, A-1040 Wien, Austria
[2] Institute of Applied Physics, University of Braunschweig, D-38106 Braunschweig, Germany
[3] Department of Chemistry, Moscow State University, Moscow, Russia
[4] Institute of Physical Chemistry, University of Vienna, A-1090 Wien, Austria

E-mail: bauer@ifp.tuwien.ac.at

Received 23 December 2004, in final form 16 February 2005
Published 11 March 2005
Online at stacks.iop.org/JPhysCM/17/1877

Abstract

Novel representatives $REPt_3Si$ (RE = La, Pr, Nd, Sm and Gd) of the $CePt_3B$ type have been synthesized and characterized by means of Rietveld x-ray powder diffraction. Measurements of the magnetic susceptibility, isothermal magnetization, temperature dependent specific heat as well as temperature and field dependent resistivity were employed to derive basic information on the low temperature behaviour. Long range antiferromagnetic order from 2.2 K ($CePt_3Si$) to 15.1 K ($GdPt_3Si$) was observed. $PrPt_3Si$, however, is non-magnetic, at least down to 400 mK, as a consequence of crystalline electric field splitting of the non-Kramers ion Pr^{3+} in tetragonal symmetry. Whilst the ordering temperature of $SmPt_3Si$ appears to be almost unaffected in external fields up to 12 T, magnetic order in $GdPt_3Si$, although twice as high as for the Sm homologue, is easily suppressed by external magnetic fields due to the absence of anisotropy.

(Some figures in this article are in colour only in the electronic version)

1. Introduction

$CePt_3Si$ ($CePt_3B$ type), as the first heavy fermion superconductor without a centre of symmetry [1], has attracted widespread attention due to distinct constrictions regarding the superconducting order parameter, which possibly give rise to a novel superconducting state [2–4]. However, not only the superconductivity but also the normal state physics of ternary $CePt_3Si$ shows a number of exceptional features. Hence, a thorough understanding of the interplay of

[5] Author to whom any correspondence should be addressed.

the superconductivity, driven by magnetic fluctuations, with the Kondo type of interaction and crystal electric field (CEF) splitting is still incomplete.

To gain more insight into general physical properties of such compounds, our studies were extended to isomorphous rare earth platinum silicides adopting the $CePt_3B$ structure type. In the course of the present study, it turned out that only compounds based on light rare earth elements (from La to Gd, except Eu) crystallize with the $CePt_3B$ structure type, whilst the heavy rare earth elements form a unique structure, which will be part of a separate study [5].

The present paper aims at a detailed investigation and evaluation of the light rare earth compounds $REPt_3Si$, to characterize the thermodynamic, electric and magnetic behaviour and work out ground states and phase transitions appearing in this series.

2. Experimental details

The starting materials used were rare earth and Pt ingots, 99.9 mass% pure, and Si pieces, 99.9999%, which were argon arc melted on a water cooled copper hearth. The arc melted buttons were vacuum sealed within thick walled quartz tubes, heat treated at 800 °C for 10 days and quenched in water.

X-ray examination and subsequent measurements of the various bulk properties for single-phase polycrystalline materials were carried out with a series of standard techniques; details are given e.g. in [6].

3. Results and discussion

3.1. Structural chemistry

Indexing of the x-ray powder patterns of $REPt_3Si$ alloys for RE = La, Pr, Nd, Sm, Gd in all cases was complete and suggested a tetragonal unit cell close to that established for $CePt_3Si$. Analysis of the x-ray intensities, systematic extinctions and sizes of unit cells suggests isotypism with the structure type of $CePt_3B$ (non-centrosymmetric space group $P4mm$—No 99) as for $CePt_3Si$ [1]. Rietveld refinements (employing the program FULLPROF [7]) with residual values generally below $R_F = 0.06$ confirmed the isotypism. As typical examples for this family of compounds, the x-ray pattern and the corresponding Rietveld profile are shown in figure 1 for $LaPt_3Si$. The minor differences between the observed (Y_{obs}) and the calculated intensity (Y_{calc}) justifies the model applied as well as guaranteeing the sample quality.

A small but significant scatter in the lattice parameters (figure 2(a) and table 1) suggests the existence of limited homogeneity regions. The volume versus rare earth dependence indicates a 3+ ground state for Ce and Sm. The monotonic variation of both a and c parameters with rising ordinal number of the rare earth agrees with a shrinking unit cell volume, i.e., the lanthanide contraction. The minor increase of the c/a ratio (compare figure 2(b)) throughout the stability range of the $CePt_3B$ structure type yields only a small increase of the lattice anisotropy. A maximal c parameter is observed for the Ce and Pr based compounds.

The structure type of $CePt_3B$ is derived from hypothetical $CePt_3$ with the cubic centrosymmetric $AuCu_3$ structure by filling the void with stabilizing boron. Whilst binary compounds {La, Ce, Eu}Pt_3 do not exist, the {Pr, Nd, Sm, Gd}Pt_3 are reported to form a $AuCu_3$-type phase; in any case incorporation of Si acts as a stabilizer forming a series of ternary compounds with a significant tetragonal distortion of the unit cell to $c/a \approx 1.34$. Figure 3 presents the structure of $REPt_3Si$ in a three-dimensional view highlighting the Pt–Si units as tetragonal bi-pyramids within the tetragonal frame of the rare earth (RE) atoms. The lack of a mirror plane perpendicular to the fourfold axis and consequently the loss of a centre of inversion is clearly seen from figure 3.

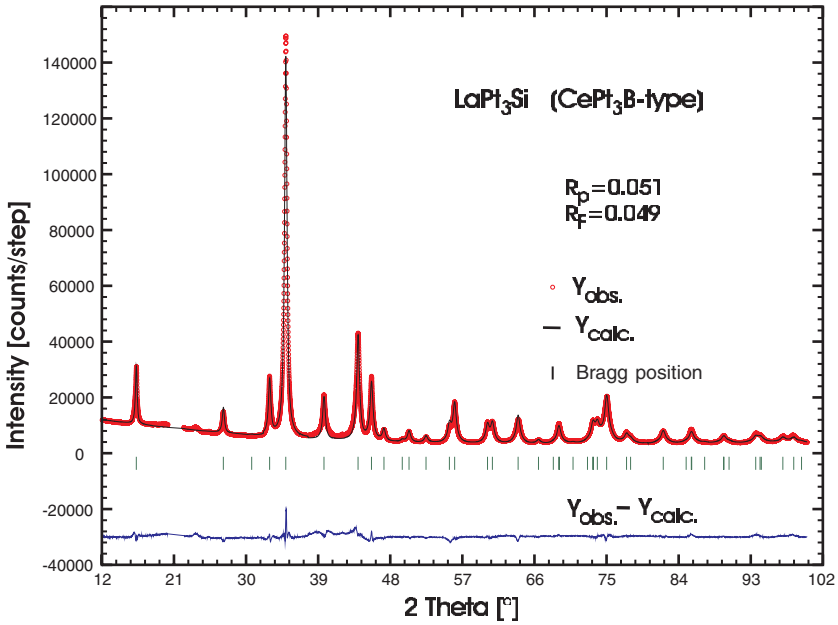

Figure 1. X-ray diffraction pattern of $LaPt_3Si$ at room temperature. The solid curve derives from a Rietveld refinement of the experimental data. $Y_{obs} - Y_{calc}$ is the intensity difference between experimental data and Rietveld calculations. The vertical bars denote the expected Bragg positions of the $CePt_3B$ type of structure.

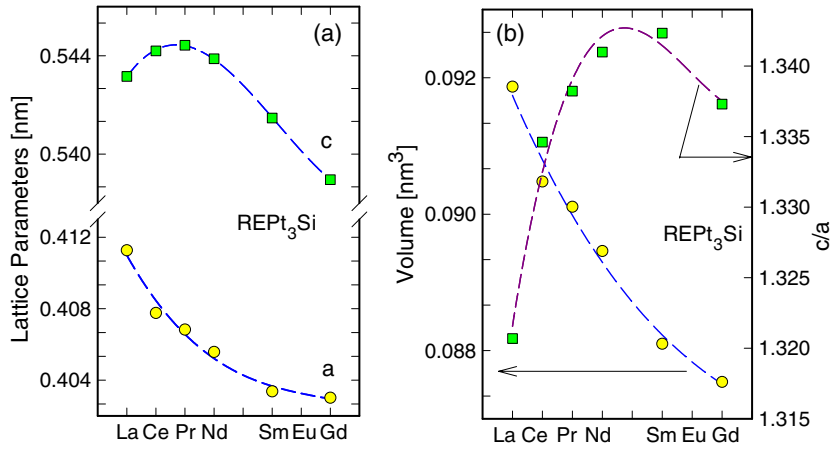

Figure 2. (a) Lattice parameter variation for light $REPt_3Si$; (b) volume and c/a ratio of light $REPt_3Si$.

Attempts to synthesize the corresponding Eu containing compound failed. Inspection by electron probe microanalysis (EMPA) for a sample with nominal composition '$EuPt_3Si$', annealed for one week at 750 °C, revealed a phase equilibrium $Eu(Pt, Si)_3 + EuPt_2Si$ instead. Similar attempts were made to synthesize corresponding compounds with Y and the heavy rare earth elements from Tb to Lu. These experiments in all cases successfully resulted in compound formation; however, different structure types were encountered. The detailed

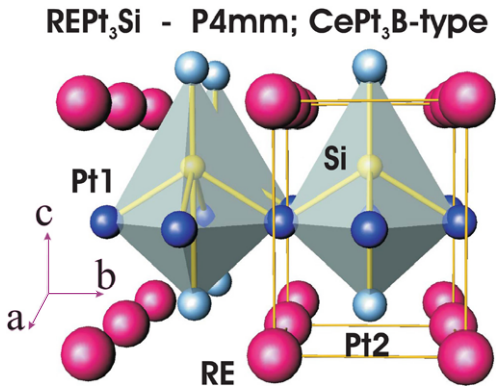

Figure 3. Crystal structure of $REPt_3Si$. Pt1 and Pt2 denote the independent crystallographic sites, 2(c) at 0.5; 0; 0.6504 and 1(a) at 0; 0; 0 (fixed). For convenient comparison with the parent $AuCu_3$ structure, the origin is shifted by (0.5; 0.5; 0.8532).

Table 1. Lattice parameters a, c, effective magnetic moment μ_{eff}, paramagnetic Curie temperature θ_p and magnetic ordering temperature T_{mag} for $REPt_3Si$.

	a (nm)	c (nm)	μ_{eff} (μ_B)	θ_p (K)	T_{mag} (K)
$LaPt_3Si$	0.411 27	0.543 16	—	—	
$CePt_3Si$	0.407 76	0.544 20	2.54	−45	2.2
$PrPt_3Si$	0.406 83	0.544 43	3.51	−15	—
$NdPt_3Si$	0.405 58	0.543 88	3.58	−7	3.3
$SmPt_3Si$	0.403 38	0.541 47	0.74	1	8.3
$GdPt_3Si$	0.403 02	0.538 96	7.73	11.5	15.1

elucidation of these slightly off-stoichiometric structures will be the subject of a forthcoming paper [8]. Structure details for $Er_{36}Pt_{102-x}Si_{32}$ were already reported in [9].

3.2. Bulk properties

In order to characterize physical features of the ternary rare earth compounds $REPt_3Si$, RE = La, Pr, Nd, Sm, Gd, temperature dependent magnetic, thermodynamic and transport properties were studied.

Figure 4(a) shows the temperature dependent magnetic susceptibility χ plotted as χ^{-1} versus T for $REPt_3Si$ with RE = Ce, Nd, Pr, Sm, Gd. Common to all the compounds investigated is a Curie–Weiss-like behaviour at elevated temperatures and anomalies at lower temperatures indicating magnetic phase transitions for Ce, Nd, Sm and Gd (compare the ac susceptibility, $\chi_{\text{ac}}(T)$, in figure 4(b)). To qualitatively account for the region above about 50 K, least squares fits according to the modified Curie–Weiss law, i.e., $\chi = \chi_0 + C/(T - \theta_p)$, were applied. χ_0 represents a temperature independent Pauli-like susceptibility, C is the Curie constant and θ_p is the paramagnetic Curie temperature. Results of this procedure are summarized in table 1. Effective magnetic moments of this series are very near to the theoretical values associated with the 3+ state of the particular rare earth ion, thereby implying rather stable magnetic moments.

The pronounced curvature of the inverse magnetic susceptibility observed for $SmPt_3Si$ follows the general trend of typical rare earth intermetallics with closely spaced multiplets.

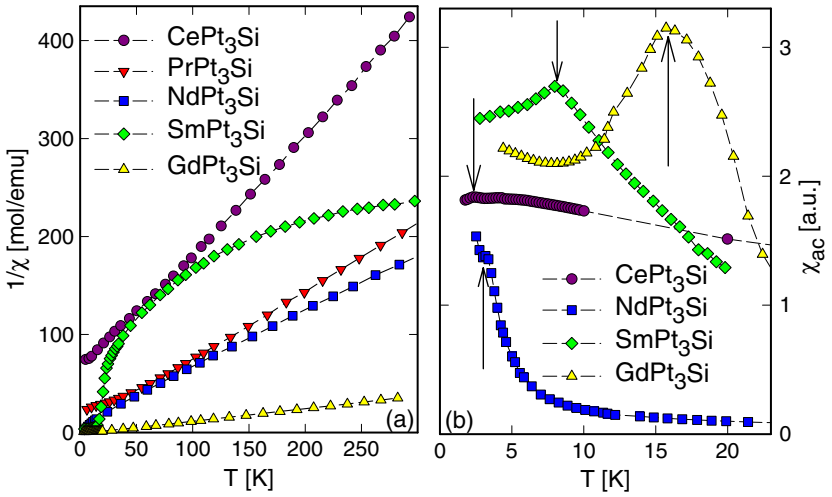

Figure 4. (a) Temperature dependent magnetic susceptibility χ plotted as $1/\chi$ versus T. (b) Details of the low temperature susceptibility χ_{ac} of $REPt_3Si$, RE = Ce, Nd, Sm, Gd. The arrows indicate the magnetic phase transition temperature. For purposes of clarity, the number of data points shown is significantly reduced (true also for figures 5–10).

No anomaly associated with a magnetic phase transition was deduced from $\chi(T)$ data for $PrPt_3Si$, at least down to 1.5 K. This, together with the levelling off of the inverse susceptibility below 30 K and an atypical deviation of the scaling behaviour of the magnetization versus the reduced field $\mu_0 H/T$, may relate to a non-magnetic ground state of the Pr ion in this tetragonal compound.

The field and temperature dependent magnetization of the Nd, Sm and Gd containing compounds allow us, in each case, to define a tentative magnetic phase diagram, T_{ord} versus $\mu_0 H$, separating the magnetically ordered regions from the field induced state.

The M/H versus T plot for $NdPt_3Si$ reveals at 2 mT a transition to weak magnetic order at $T = 3.2$ K (figure 5(a)). The antiferromagnetic nature of this transition is indicated by the linear relation of M versus H for small fields (compare the inset, figure 5(b)). A field induced transition at 0.37 T and 2 K, as a reorientation between two antiferromagnetic states (AFM I and AFM II), is obvious from the M versus H curve saturating at about 1.5 μ_B in a field of 5 T. Compared to the theoretically expected value of $g \cdot j = 3.27$ μ_B (g—Landé factor, j—total angular momentum), the experimentally saturated moment appears strongly reduced owing to CEF effects. Inspection of the M/H versus T dependence (figure 5(a)) shows for a narrow range of fields (0.1–0.4 T) a twofold transition from AFM I to AFM II followed by a field induced transition towards ferromagnetism. The field dependences of both transitions are summarized in terms of a magnetic phase diagram in figure 5(b).

The temperature dependent magnetization of $SmPt_3Si$ for various fields (not shown here) is indicative of antiferromagnetic order, confirmed from Arrott plots of M^2 versus H/M. Although small magnetic moments are involved, there is little temperature dependence in the ordering temperature in fields up to 6 T. The origin of this observation may be seen in a significant magnetic anisotropy associated with the localized Sm moments.

In contrast to the Sm case, a substantial temperature dependence of the antiferromagnetic ordering temperature of $GdPt_3Si$ is seen from the M/H versus T data (figure 6(a)). The phase diagram linked with these results is shown in figure 6(b). Again, Arrott plots confirm the antiferromagnetic ground state.

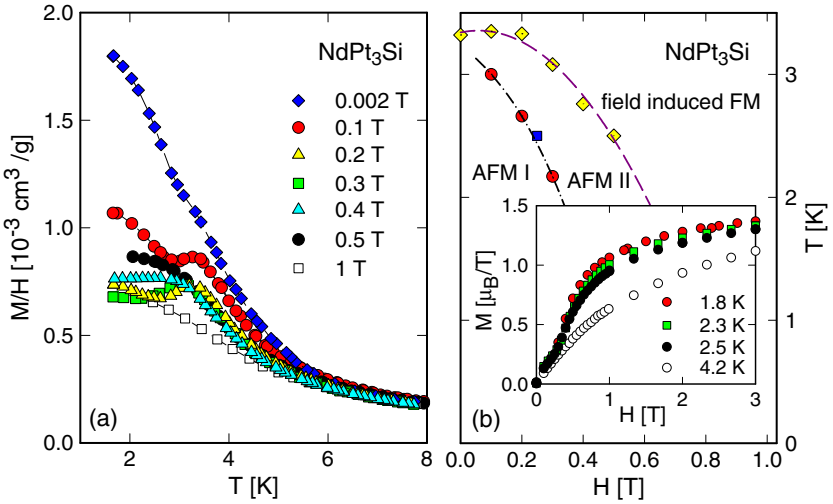

Figure 5. (a) Temperature dependent M/H curves of $NdPt_3Si$ at various fields. (b) Magnetic phase diagram of $NdPt_3Si$. The inset shows isothermal M versus $\mu_0 H$ data.

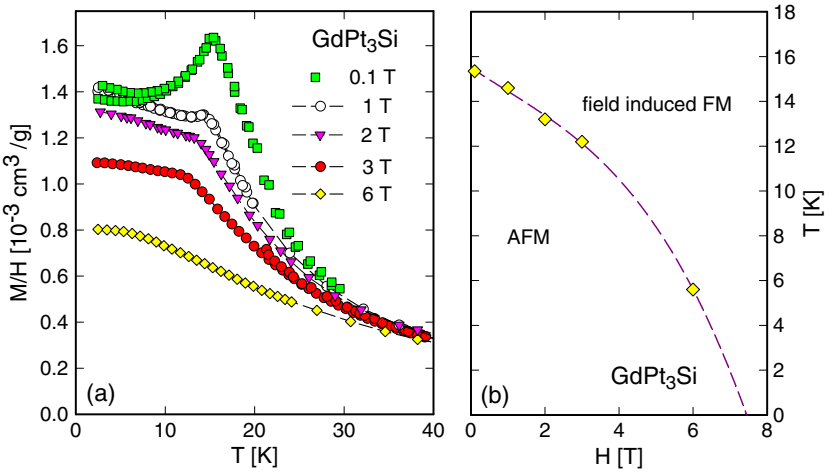

Figure 6. (a) Temperature dependent M/H curves of $GdPt_3Si$ at various fields. (b) Magnetic phase diagram of $GdPt_3Si$.

Figure 7 displays the temperature dependent specific heat C_p of the title compounds. In good agreement with magnetization data, ordering is observed from λ-like anomalies in the case of RE = Ce, Nd, Sm, Gd at 2.2, 3.3, 8.3 and 15.1 K respectively. No magnetic phase transition, at least down to 1.5 K, was encountered for $PrPt_3Si$, confirming the $\chi(T)$ measurement. In order to obtain the magnetic contribution to $C_p(T)$, data on isostructural non-magnetic $LaPt_3Si$ are subtracted from the individual specific heat curves. Results are shown as C_{mag}/T versus T in figure 8.

The type of phase transition as well as the behaviour within the ordered state fully comply with simple mean field theory. Quantitatively, the magnetic contribution to the specific heat

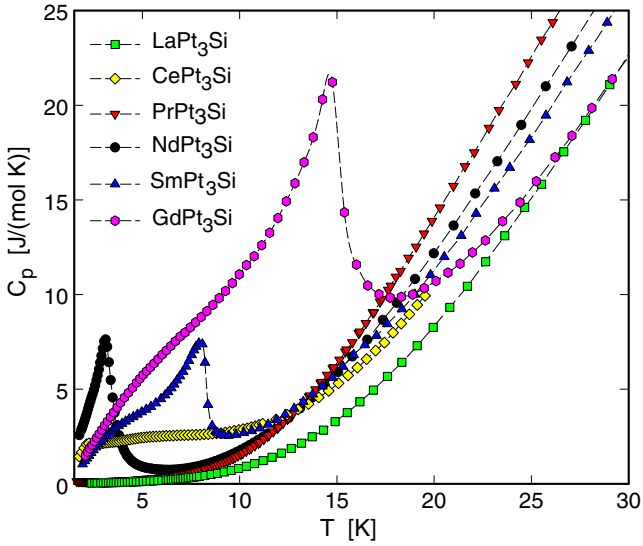

Figure 7. Temperature dependent specific heat C_p for light $REPt_3Si$.

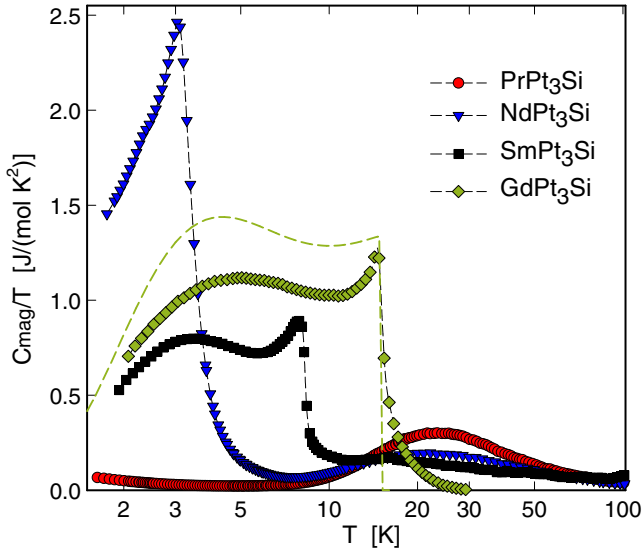

Figure 8. Temperature dependent magnetic contribution to the specific heat, C_{mag}, for $REPt_3Si$ plotted as C_{mag}/T versus T. The dashed curve is a mean field calculation for $GdPt_3Si$.

can be expressed as

$$C_{mag}(T) = -\frac{1}{2}\gamma\frac{\partial(M^2)}{\partial T} - H_{ext}\frac{\partial M}{\partial T}, \tag{1}$$

where γ is the molecular field parameter, M is the magnetization calculated in terms of the mean field model and H_{ext} is an externally applied magnetic field. The second part of equation (1) vanishes, however, in the field free case. $GdPt_3Si$ is the best example, as due to the $j = 7/2$ state (with orbital angular momentum $l = 0$) no CEF effect is present. Within this theory, the

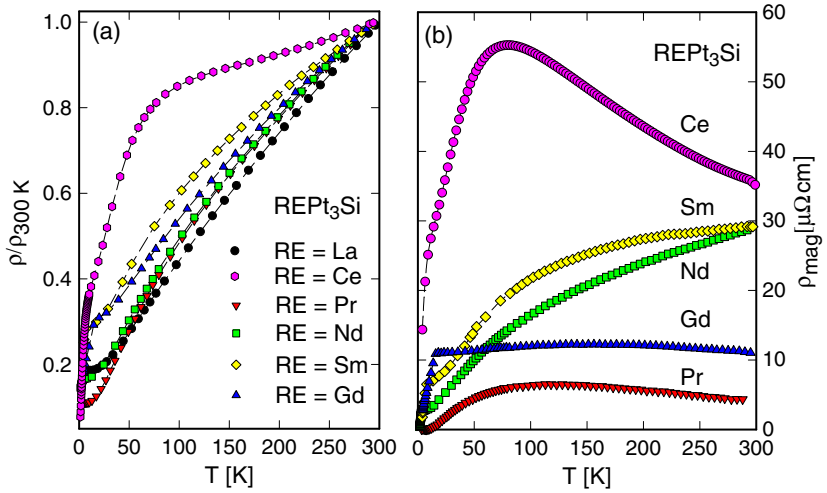

Figure 9. (a) Normalized temperature dependent electrical resistivity ρ/ρ_{RT} for light $REPt_3Si$. For clarity, only each tenth data point is displayed. (b) Temperature dependent magnetic contribution to the electrical resistivity ρ_{mag} of $REPt_3Si$ (see the text).

jump of the specific heat anomaly at $T = T_{mag}$ follows from

$$\Delta C_{mag}(T = T_{mag}) = 5R\frac{j(j+1)}{2j^2+2j+1} \tag{2}$$

where R is the gas constant. Values according to equation (2) are 20.37, 19.66 and 20.14 J mol^{-1} K^{-1}, for the Nd, Sm, Gd compounds, respectively. Whilst the Gd compound closely follows the mean field results ($\Delta C_{mag} \approx 18.8$ J mol^{-1} K^{-1}), the compounds containing Ce (well below 1 J mol^{-1} K^{-1}), Nd ($\approx$7.6 J mol^{-1} K^{-1}) and Sm ($\approx$7.6 J mol^{-1} K^{-1}) significantly deviate from the theoretical values. This indicates that magnetic order does not arise from the total angular momentum associated with Hund's rules; rather, CEF effects in tetragonal symmetry cause a lifting of the $(2j+1)$-fold ground state degeneracy. Accordingly, the ground state level will be a magnetic doublet in the case of Kramers ions, i.e., Ce, Nd and Sm. In fact, the entropy gain $S_{mag} \approx R \cdot \ln 2$ (R—gas constant) at the ordering temperature of the Nd and the Sm compound corroborates a doublet as ground state. Additionally, Kondo-type interactions in the case of $CePt_3Si$ further reduce the specific heat jump at $T = T_{mag}$ [1].

The pronounced shoulder in the heat capacity of $GdPt_3Si$ on the low temperature side of T_{mag} can be explained in mean field theory by Zeeman splitting of the $j = 7/2$ state owing to the strong molecular field. Assuming next nearest neighbour interactions with a molecular field constant $\lambda = 0.191\ \mu_B/T$ fairly well reproduces T_c and the aforementioned shoulder of the magnetic contribution to the specific heat.

The temperature dependent electrical resistivity $\rho(T)$ of the light rare earth silicides $REPt_3Si$ is plotted in figure 9(a) in a normalized representation. The room temperature resistivity values are 57.3, 88.3, 57.7, 86.7, 98.7 and 66.8 $\mu\Omega$ cm, for RE = La, Ce, Pr, Nd, Sm and Gd, respectively. Whilst all these samples are metallic in the temperature range investigated, $TmPt_3Si$—although crystallizing in a derivative structure type—reveals a negative temperature coefficient of the electrical resistivity below room temperature [10]. Magnetic order for Nd, Sm and Gd is reflected by a drop in $\rho(T)$ below 3.2, 7.5 and 15 K, respectively, in perfect agreement with specific heat and susceptibility data. Low temperature features of $REPt_3Si$ are shown in more detail in figure 9.

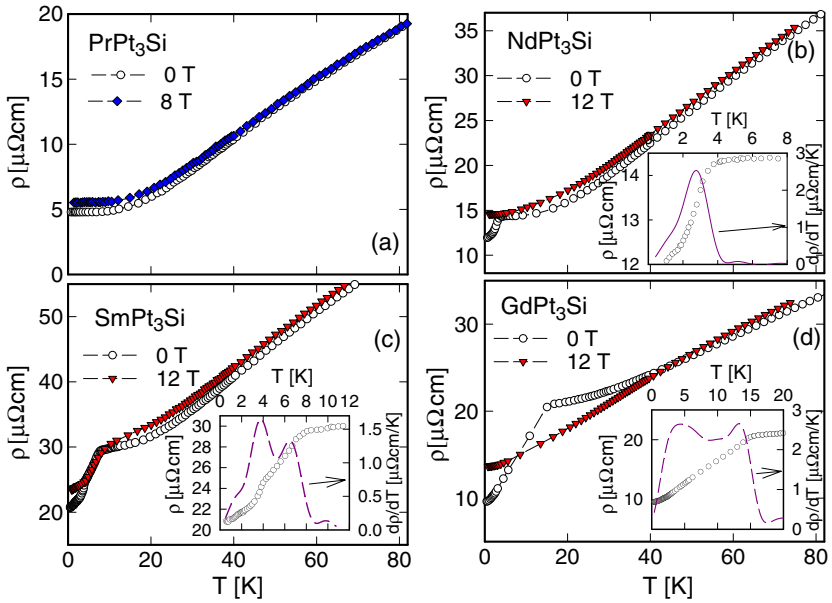

Figure 10. Low temperature part of the temperature and field dependent electrical resistivity of (a) PrPt$_3$Si, (b) NdPt$_3$Si, (c) SmPt$_3$Si and (d) GdPt$_3$Si. The insets show resistivity details around the ordering temperatures together with their temperature derivatives.

The interaction of conduction electrons with the magnetic moments of the light rare earth ions causes an additional contribution to the electrical resistivity, $\rho_{\rm mag}$. In the absence of CEF effects and well above the overall CEF splitting, $\rho_{\rm mag}(T)$ is temperature independent [11]. The thermal population of the individual CEF levels, however, gives rise to new scattering channels. As a consequence, pronounced temperature dependences may result for $\rho_{\rm mag}(T)$. The particular behaviour of $\rho_{\rm mag}(T)$ for a specific compound depends on the energy separation between CEF levels, as well as on the matrix elements connecting the states involved [11]. Experimentally, $\rho_{\rm mag}(T)$ is obtained by subtracting from the total measured effect of REPt$_3$Si both the phonon part (taken from non-magnetic LaPt$_3$Si) as well as the respective residual resistivities. Results of such an analysis are displayed in figure 9(b). Above $T_{\rm mag}$, $\rho_{\rm mag}(T)$ of GdPt$_3$Si appears to be almost temperature independent, in line with the $j = s = 7/2$ state of the Gd^{3+} ion, where the spherical distribution of the 4f charge density prevents CEF splitting. Moreover, this experimental result evidences that the phonon part, as defined by LaPt$_3$Si, properly represents this contribution for REPt$_3$Si. It should be noted that this conclusion is also corroborated by the heat capacity (compare figure 7), where the data on LaPt$_3$Si and GdPt$_3$Si match slightly above the phase transition temperature. The remaining compounds of the present series exhibit pronounced curvatures of $\rho(T)$ caused by CEF effects. Finally, the distinct behaviour of CePt$_3$Si in the paramagnetic temperature range is attributed to Kondo interaction in the presence of strong CEF splitting [1].

The low temperature features of the electrical resistivity and its field dependence are displayed in figure 10. $\rho(T)$ for PrPt$_3$Si exhibits a rather smooth temperature dependence without any sign of magnetic order down to about 400 mK. These data support the conclusion derived from specific heat and magnetic susceptibility of a non-magnetic ground state of the Pr^{3+} ion. In consequence, a fit of the simple Bloch–Grüneisen law to $\rho(T)$ up to about 100 K reveals excellent agreement, indicating that scattering of conduction electrons on the localized moments of Pr does not produce significant temperature dependence. The Debye temperature

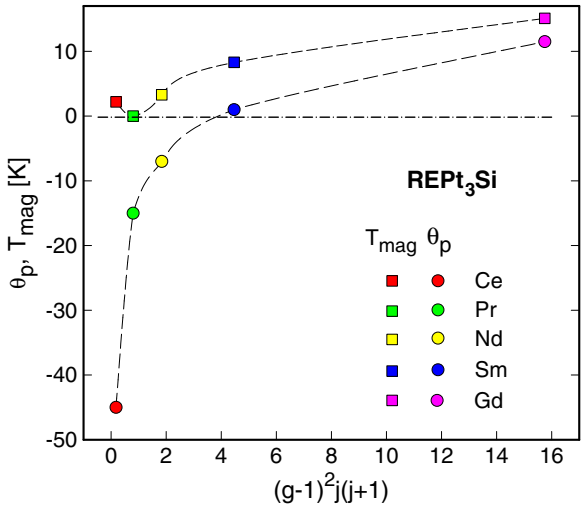

Figure 11. Correlation of the ordering temperature T_{mag} and the paramagnetic Curie temperature θ_{p} with the de Gennes factor $(g-1)^2 j(j+1)$ for the light $REPt_3Si$.

derived ($\theta_{\mathrm{D}} \approx 110$ K), however, seems to be unphysically low. The application of a magnetic field causes a positive magnetoresistance, in line with the classical behaviour of metals.

A non-magnetic ground state in Pr based compounds is frequently observed and can be understood in terms of the CEF driven lifting of the $2j + 1 = 9$-fold degeneracy of the Pr^{3+} ion. In context with the tetragonal symmetry ($P4mm$) the ninefold-degenerate ground state splits into a sequence of levels comprising singlets and doublets. The particular distribution of levels as well as their degeneracies strongly depend on the set of CEF parameters. Since a description of Pr in tetragonal symmetry requires five CEF parameters, a fit of the van Vleck formula to polycrystalline susceptibility is unfeasible. Either single-crystal or neutron inelastic scattering data are thus necessary in order to obtain detailed information about the CEF effect in this series. However, the overall CEF splitting needs to be small to comply with the Pr^{3+} state derived from $\chi(T)$ data above about 100 K.

The primary feature of $\rho(T)$ of $NdPt_3Si$ is the onset of magnetic order at $T_{\mathrm{ord}} = 3.2$ K (compare the inset of figure 10(b)), in good agreement with the specific heat and susceptibility measurements. A positive magnetoresistance is observed in the temperature range studied for external fields of 12 T, where the anomaly associated with the magnetic phase transition is suppressed.

A kink in $\rho(T)$ of $SmPt_3Si$ around 7.5 K evidences magnetic order (figure 10(c)). A weaker anomaly around 4 K may be indicative of a modification of the spin structure of the Sm moments (inset, figure 10(c)). While the onset of magnetic order is seen from both specific heat and susceptibility, the reorientation becomes evident only in the $\rho(T)$ study. Additionally, the application of an external magnetic field seems to shift the onset of magnetic order to higher temperatures and would thus imply a predominantly ferromagnetic transition.

Magnetic order in the case of $GdPt_3Si$ is observed around 15 K (figure 10(d) and inset), again in good agreement with specific heat and susceptibility. In contrast to the Sm compound case, magnetic order is suppressed in external fields of 12 T, although the magnetic ordering temperature is almost twice as large as for $SmPt_3Si$. This feature can be taken as a sign of antiferromagnetic order with vanishing anisotropy.

Neither the paramagnetic Curie temperature θ_{p} nor the ordering temperature T_{mag} seems to correlate with the de Gennes factor (compare figure 11), as expected for simple localized

magnetic systems. Deviations may result mainly from two mechanisms: (i) CEF effects, (ii) the presumably non-magnetic ground state of the non-Kramers ion Pr. As regards (i), one has to consider that de Gennes scaling relates to the total angular momentum j of a certain rare earth element. The symmetry of the crystal together with the particular value of j, however, defines the ground state and magnetic ordering, thereby modifying the wavefunctions of the unperturbed state associated with j. As a consequence, the ordering temperature is, in general, smaller than that extrapolated from Gd, where no CEF applies. As a matter of fact, the Ce system, affected by Kondo interaction, does not comply with the de Gennes factor. (ii) The tetragonal crystal symmetry in the context of the $j = 4$ total angular momentum of Pr^{3+} provides the basis for various CEF multiplets without a resulting magnetic moment. Due to these CEF effects, a non-magnetic ground state results in $PrPt_3Si$, although the Pr moment is, in principle, large.

Similar arguments may hold for the paramagnetic Curie temperature θ_p. Figure 11 shows a non-linear but monotonic rise of θ_p when proceeding from Ce to Gd. Whilst the early rare earths, Ce, Pr and Nd, exhibit a negative value of θ_p, indicative of antiferromagnetic interactions, both Sm and Gd show positive θ_p as a fingerprint of ferromagnetic correlations. For Ce and Nd containing compounds, the negative θ_p is in perfect agreement with the experimentally observed type of magnetic order; ferromagnetic correlations for the Sm and Gd containing compounds seem to be too weak to compete with the experimentally observed antiferromagnetic state.

4. Summary

Ternary $REPt_3Si$ compounds with RE = La, Ce, Pr, Nd, Sm and Gd were synthesized by arc melting and found to crystallize in the tetragonal $CePt_3B$ structure with the non-centrosymmetric space group $P4mm$. Besides superconductivity in $CePt_3Si$ at $T_c = 0.75$ K, long range antiferromagnetic order was encountered for RE = Ce, Nd, Sm and Gd. $PrPt_3Si$ does not show any sign of long range magnetic order down to 400 mK, due to a non-magnetic CEF ground state arising for the non-Kramers Pr^{3+} ion in tetragonal symmetry. A mean field type of order is derived and explicitly verified in the spin-only case $GdPt_3Si$. CEF effects are conceived to be responsible for the observed deviation of the magnetic ordering temperatures from a de Gennes scaling. Although the paramagnetic Curie temperature exhibits a crossover from negative to positive values with increasing ordinal numbers of rare earths, which generally signifies a transition from antiferromagnetic to ferromagnetic interaction, the ground state remains antiferromagnetically ordered throughout the series. On the basis of the RKKY type of magnetic interaction, interatomic rare earth distances seem to be consistent with negative exchange values of the oscillating RKKY function.

Acknowledgments

This research was sponsored by the Austrian FWF under grants P16370 and P15066. The authors are grateful to the OEAD for support within the framework of the Austrian–Russian bilateral exchange programme within project I.18/4 and RFBR 03-03-20001BNTS-a.

References

[1] Bauer E, Hilscher G, Michor H, Paul Ch, Scheidt E W, Gribanov A, Seropegin Yu, Noel H, Sigrist M and Rogl P 2004 *Phys. Rev. Lett.* **92** 027003

[2] Yogi M, Kitaoka Y, Hashimoto S, Yasuda T, Settai R, Matsuda T D, Haga Y, Onuki Y, Rogl P and Bauer E 2004 *Phys. Rev. Lett.* **93** 027003

[3] Samokhin K V, Zijlstra E S and Bose S K 2004 *Phys. Rev.* B **69** 094514
[4] Frigeri P A, Agterberg D A, Koga A and Sigrist M 2004 *Phys. Rev. Lett.* **92** 097001
[5] Rogl P *et al* 2005 to be published
[6] Bauer E, Berger St, Paul Ch, Della Mea M, Hilscher G, Michor H, Reissner M, Steiner W, Grytsiv A, Rogl P and Scheidt E W 2002 *Phys. Rev.* B **66** 214421
[7] Roisnel T and Rodriguez-Carvajal J 2001 *Mater. Sci. Forum* **378–381** 118
[8] Gribanov A *et al* 2005 to be published
[9] Tursina A I, Gribanov A V, Noel H, Rogl P and Seropegin Y D 2004 *Acta Crystallogr.* E **60** i8 (Structure Reports)
[10] Bauer E *et al* 2005 to be published
[11] Rao V U S and Wallace W E 1970 *Phys. Rev.* B **2** 4613